Journal of Materials Chemistry C

Accepted Manuscript

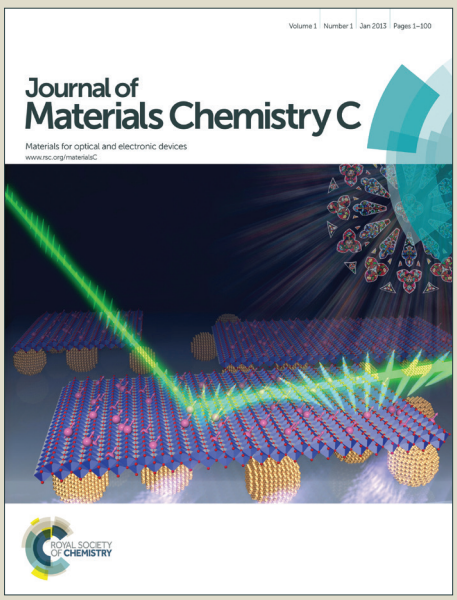

ROYAL SOCIETY OF CHEMISTRY

www.rsc.org/materialsC

High-Performance ZnO/Ag Nanowires/ZnO Composite Film UV Photodetectors with Large Area and Low Operating Voltage

Zhi Yang,[a] *Minqiang Wang,*[a,*] *Xiaohui Song,*[a] *Guodong Yan,*[a]

Yucheng Ding,[b] *and Jinbo bai*[c]

[a]Electronic Materials Research Laboratory (EMRL), Key Laboratory of Education Ministry; International Center for Dielectric Research, Xi'an Jiaotong University, Xi'an, 710049, China.

[b]State Key Laboratory of Manufacturing Systems Engineering, Xi'an Jiaotong University, Xi'an 710049, China.

[c]Laboratory MSSMat, UMR CNRS8579, Ecole Central Paris, 92290 Chatenay-malabry, France.

Corresponding Author:

[*]E-mail: mqwang@mail.xjtu.edu.cn. Tel: +86-29-82668794;

Abstract : A simple and low-cost solution-processed method is used to fabricate ZnO/Ag nanowires/ZnO composite UV photodetectors with large area of 4×5mm^2, low operating voltage of 1 V and high visible transmittance of 75%. Due to the low-dimensionality confine ability and little persistent photoconductivity effect in polycrystalline ZnO nanoparticles thin films, and excellent conductivity of Ag nanowires network, composite UV photodetectors exhibit high on/off ratio and short response time under high light illumination, while large detectivity and responsivity under low light illumination. Compared with traditional polycrystalline ZnO thin films, the formation of a large number of Ohmic contacts between ZnO nanoparticles and Ag nanowires in composite structure greatly improves the extraction number and

shortens extraction time of photoelectrons. Additionally, both Schottky contact and Ohmic contact at the electrode interface can obtain high on/off ratio and short response time. Our composite structure device is regarded as a compromise between high-performance with large-area, low-voltage and low-cost. It has many advantages compared with its counterparts include ZnO nanowire, and other ZnO composites, which is very promising in UV photodetective applications.

Keywords: Polycrystalline ZnO thin films; Ag nanowires; composite structure UV photodetectors; high performance; large area; low voltage

1. Introduction

For decades, UV photodetectors have been widely used in many applications such as flame sensing, environmental research, astronomical study, optical communication, and so on.[1] Across all application areas, several critical performance parameters for UV photodetectors include responsivity, response time, and detectivity.[2] For example, for flame sensing application, high responsivity of 0.1 A/W, short response time of 1~3 s, and high detectivity of 10^{11} Jones are necessary to UV photodetectors based on photoconductor type.[3] Besides, some requirements such as large photosensitive area, low operating voltage, room temperature operation, simple processing condition, and low-cost integration are also necessary to practical applications. Compared with commercial silicon photodiodes, UV photodetectors based on wide bandgap semiconductors have received more and more attentions due to their intrinsic visible-blindness and enable room-temperature operation.[4] In particular, ZnO has great potential in UV detection due to its large bandgap of 3.35 eV at room

temperature, and various synthetic methods. Solution-processed method can produce ZnO thin films with large area and different morphology including nanoparticles (NPs), nanorods (NRs) and nanowires (NWs), which is very flexible and low cost. Besides, Tian et al reported ZnO-SnO_2 heterojunction nanofibers UV photodetectors with high performance based on electrospun process, which is another excellent method to produce large-scale nanofiber film with low cost. [5]

ZnO NWs UV photodetectors have been studied widely due to their high on/off current ratio, and fast response and recovery speeds.[6, 7] Previously, Su et al fabricated vertical ZnO NWs arrays UV photodetectors using hydrothermal method.[8] Furthermore, their group fabricated laterally aligned ZnO nanobridge UV photodetectors to improve responsivity and shorten recovery time.[9] Besides, Bai et al demonstrated that integrating multiple ZnO NWs connected in parallel was an effective approach to fabricate large-scale flexible NWs photodetectors with high on/off ratio.[7] However, compared with ZnO NWs, ZnO NPs with reduced dimensionality can confine the active area of the charge carrier better.[10] Additionally, ZnO NPs thin films have little persistent photoconductivity (PPC) effect,[8] which means the photocurrent persists for a long time after the light is shut off. This PPC effect often appears in ZnO NWs photodetectors[8, 11-13] and GaN-based devices[14]. Even so, the polycrystalline nanoparticles thin films still have the shortcoming of poor conductivity. Thus high operating voltage is required to get large photocurrent. For example, Jin et al reported that the photocurrent of ZnO NPs UV photodetector reached 310 μA only when 120 V bias was applied.[1] Our previous research also

indicated that 30 V bias was needed for PbSe[15] and PbTe[16] NPs thin films. This operating voltage may be too high to meet the requirement of low power and easy integration. In order to overcome poor conductivity and further improve the performance of photodetectors, many ZnO composite UV photodetectors based on Ag NWs,[17] Ag NPs,[18] Au NPs,[19] graphene[20, 21] and single-walled carbon nanotubes (SWNTs)[10] have appeared.

Among many methods to improve performance of polycrystalline ZnO NPs thin films UV photodetector, we particularly expect to build a conductive network buried in ZnO NPs thin films, and further create excellent Ohmic contact between ZnO NPs and conductive network so that a large number of conductive paths can be created in the composite thin films. After doing this, the photoelectrons in ZnO NPs can be transferred to electrodes, and be extracted to the external circuit rapidly. As well known, Ag NWs thin films can act as transparent electrodes in solar cells and flat panel display due to their high conductivity and optical transmittance.[22-24] So if Ag NWs can be buried in ZnO NPs thin films, this will not only greatly improve the extraction number of photoelectrons, but also shorten extraction time in polycrystalline thin films. Then no doubt the high responsivity and short response time will be achieved.

In this paper, the ZnO/Ag NWs/ZnO composite UV photodetectors were fabricated as the process in Experimental details. Several measurements include optical transmittance, IV characteristic and time-dependent photoresponse have been conducted for composite UV photodetectors fabricated at different processing

condition. Then some performance parameters include photocurrent, on/off ratio, responsivity, detectivity, response and recovery time could be obtained. The results indicate that ZnO/Ag NWs/ZnO composite UV photodetectors with large active area of 4×5 mm^2 prepared by optimized process exhibit excellent UV photodetective performance. So our strategy can be comparable with hybrid PbS quantum dots (QDs)/grapheme IR photodetector with ultrahigh responsivity,[25, 26] which depends on rapid transfer of holes from PbS QDs to grapheme.

2. Results and discussion

The structure of ZnO/Ag NWs/ZnO composite UV photodetector is depicted in Fig. 1a. The three layers structure like sandwich includes bottom ZnO NPs thin film, middle Ag NWs network, and upper coated ZnO NPs layer. The size of bottom ZnO NPs is about 20 nm (Fig. S1a). From Fig. 1b, we can see Ag NWs through the compact upper ZnO NPs layer clearly, indicating very thin layer of upper ZnO NPs. Fig. S2 shows XRD and TEM analysis of three layers. Besides, Fig. 1c shows that Ag NWs junctions are totally coated with upper ZnO layer, which demonstrates that conductive network is buried in ZnO NPs layer, and good contact can be created between Ag NWs and ZnO NPs. In addition, the coated layer of upper ZnO can not only greatly increase contact area between Ag NWs and ZnO NPs, but also play a role in protecting Ag NWs from physical scratch, which has been tested in ref 22. From magnified area in Fig. S3, the electrode gap is 4 mm, and Ag NWs network can be built across the entire electrode gap. From cross section of device in Fig. 1d,

combined with Fig. S1b, the three layers structure and very thin layer of upper ZnO NPs can be further confirmed.

In order to verify the effectiveness of this device structure, we compared the IV characteristic of two UV photodetectors (Fig. 2a), ZnO/Ag NWs/ZnO composite films and two layers ZnO NPs thin films without middle Ag NWs layer. The Ag electrodes with gap of 4 mm were firstly chosen to rule out the impact of electrodes contact. The symmetrical and linear characteristic of IV curve confirms the Ohmic contact between Ag NWs and ZnO NPs. Under the light illumination of 10μW/cm^2, ZnO/Ag NWs/ZnO composite film UV photodetector has photocurrent of 4.7 μA, while ZnO NPs thin film only has 0.08 μA. Besides, the photoresponse times of two UV photodetectors are 16 s (Fig. 3d) and 74 s (Fig. S4), respectively. This great difference demonstrates that middle Ag NWs network plays a role in rapidly transferring photoelectrons in ZnO NPs to electrodes. Even though, the performance of composite UV photodetector has a close relationship with the Ag NWs density. When Ag NWs films are spin-coated from the Ag NWs ink with given concentration, the lower spin speed will produce denser Ag NWs films, which can be confirmed in Fig. S5. The dependence of photocurrent and on/off ratio on spin speed of Ag NWs can be described in Fig. 2b. The photocurrent shows a monotonically increase as decreased spin speed of Ag NWs. Besides, when spin speed of Ag NWs is 1500 rpm, on/off ratio of device can reach 313, which is much larger than the remaining three devices. The similar feature can be occurred for another parameter, thickness of bottom ZnO layer. When the procedure of bottom ZnO layer is repeated twice, corresponding to

the thickness of 85 nm, the largest on/off ratio is 40 (Fig. 2c). Based on these experiment results, we can find that too much Ag NWs and bottom ZnO layer have large photocurrent but low on/off ratio. So we define that optimized processing condition of ZnO/Ag NWs/ZnO composite UV photodetector is bottom ZnO layer with thickness of 85 nm, Ag NWs films with spin speed of 1500 rpm, and a thin layer upper ZnO NPs. Another important point to UV photodetector is the wavelength-dependent responsivity, indicating spectral selectivity of photoresponse, which is quite related to transmittance of composite thin films at different wavelength. From Fig. 2d, all thin films have nearly the same UV transmittance at shorter than 380 nm of wavelength, and the thin films without Ag NWs have the largest visible transmittance around 85% (at 550 nm). Besides, the lower spin speed of Ag NWs produces smaller visible transmittance, corresponding to denser Ag NWs network, which is in accordance with above results. In addition, we find that there is the same optical transmittance for composite thin films with and without upper ZnO NPs, which confirms the very thin layer of upper ZnO NPs. If upper ZnO layer is too thick, both the conductivity and transmittance of composite films will decrease.

To get a better understanding of the photodetective mechanism, we investigated the IV curves of ZnO/Ag NWs/ZnO composite UV photodetector with optimized processing condition under different light illumination (Fig. 3a). The IV curves are symmetrical and linear as previous discussed. One figure of merit for photodetectors is linear dynamic range (LDR),[27] which can be expressed by

$$LDR = 20\log(J_{ph} / J_{d}) \quad (1)$$

where J_{ph} and J_d are the photocurrent and dark current, respectively. Fig. 3b summarizes the obtained photocurrent at 1 V bias from Fig. 3a versus the light illumination. The largest photocurrent is 41.8 μA under the light illumination of 4.9mW/cm^2. Besides, under the light illumination of 1mW/cm^2, the calculated LDR is 64 dB, which is very close to InGaAs photodetectors (66 dB).[27, 28] In addition, the detectivity D* is commonly reported as important parameter to describe sensitivity of photodetectors.[29] Based on Gong's discussion,[28] if shot noise from the dark current is the major contributor to the total noise, D*can be simplified expression as

$$D^*(\text{cm Hz}^{1/2}\ \text{W}^{-1}\ \text{or Jones}) = (J_{ph}/AE_i)/(2qJ_d)^{1/2} \quad (2)$$

where q is electronic charge, A is the active area, and E_i is the light intensity. The calculated detectivity as function of light illumination is plotted in Fig. 3b. The calculated values of detectivity change from 10^{11} to 10^{13} Jones. In particular, the largest detectivity is 6.8×10^{12} Jones at 1 V bias under the light illumination of 10μW/cm^2, indicating excellent weak light detection capability of composite UV photodetectors, which is comparable with that of PbS colloidal QDs IR photodetector (1.5×10^{12} Jones)[30] and composite PbSe dual wavelength photodetector (3×10^{13} Jones)[27]. This result further verifies the structure advantage of ZnO/Ag NWs/ZnO composite UV photodetector. The Ag NWs embedded in polycrystalline ZnO NPs thin films develop the excellent role of transferring electrons to improve the output of photoelectrons, which even can comparable with single crystalline ZnO schottky photodiodes fabricated by MOCVD technique.[31] Table 1 summarizes the various reports about ZnO UV photodetectors in comparison with our experimental results.

The time-dependent measurements of photoresponse were employed to study the response and recovery time. The response time τ_r, usually define as the time to approach 63% of the maximum photocurrent, and the recovery time τ_d, is the time to decay to 37% of the maximum photocurrent.[20] We fitted the rising and decay curves using exponential function in Fig. 3c. Under the light illumination of 4.9mW/cm^2, the response and recovery times are 3.53 s and 3.67 s, respectively, and there is no PPC effect. This response and recovery times are much shorter than most reported polycrystalline ZnO NPs photodetector, whose response time can ranging from minutes to hours.[32, 33] Furthermore, time-dependent photoresponse under different light illumination was plotted in Fig. 3d, indicating prolonged response and recovery times with decreasing light illumination, which is in accordance with other's results.[34] All above good results for ZnO/Ag NWs/ZnO composite UV photodetector come from the interaction between Ag NWs and ZnO NPs. When ZnO NPs come into contact with Ag NWs, electrons will flow from Ag NWs to ZnO NPs to establish a uniform Fermi energy level, and the space charge layer can form at the interface.[17] Fig. 4a describes energy band structure of forming heterojunction between Ag NWs and ZnO NPs. The formed downward bending of ZnO conduction band suppresses the recombination of excitons under light illumination, allowing more photoholes discharging the trapped electrons at the surface states of ZnO NPs while accelerating the movement of photoelectrons toward the Ag NWs. Next, we will explain the photoresponse of ZnO based on adsorption and desorption of oxygen molecules on the surface. The ZnO NPs have the advantage of very large surface to volume ratios,

which facilitate the adsorption and desorption of oxygen molecules. The oxygen molecules are adsorbed on the surface by capturing free electrons in ZnO NPs to create the depletion regions, producing the high-resistance in nanocrystal films (100 MΩ in our experiments). When exposed to photons with energy higher than E_g of ZnO, electron-hole pairs are generated (Fig. 4b). The photoholes can migrate to the surface along the potential gradient and recombine with the O_2^- trapped electrons, thus releasing O_2 from the surface. The remaining photoelectrons can be transferred to the Ag NWs rapidly with the help of formed heterojunction. Then a large number of photoelectrons can be transferred to electrodes by Ag NWs conductive network as "highway". When the light is shut off, oxygen molecules readsorb on the ZnO NPs surfaces by capturing photoelectrons. On the other aspect, photoelectrons can return to ZnO NPs rapidly from Ag NWs for recombination due to the good Ohmic contact, which avoids the PPC effect effectively. The PPC effect usually appears because electrons have to cross barriers around grain boundaries prior to recombination, which increases the recovery time.[2, 8, 12]

The electrode contact is quite important for the performance of detectors. Using Schottky contact has been believed to increase sensitivity and the response and recovery speeds, since the strong electric field at the reversely biased Schottky barrier area can separate the photogenerated excitons rapidly.[35, 36] The Ag and Al electrodes are usually used to study the Ohmic contact with ZnO,[7, 37, 38] while Au electrode is for Schottky contact.[1, 39] As a comparison with Ag electrode used above, Fig. 5a and 5b show the IV curves of ZnO/Ag NWs/ZnO composite UV photodetector with Al and

Au electrodes under different light illumination, respectively. Al contact produces symmetrical and linear IV characteristics, while Au contact shows clear non-symmetrical. Besides, the photocurrent of Al contact is almost ten times of Au contact. These results demonstrate the intrinsic Ohmic contact for Al electrodes and Schottky contact for Au electrodes. Another parameter to UV photodetectors is responsivity (R), which is defined as

$$R(\mathrm{A/W}) = J_{ph} / AE_i = \alpha E_i^{\beta-1} \quad (3)$$

where α and β are fitting parameters of exponential function.[25, 40] Fig. 5c compares the responsivity of composite UV photodetectors versus light illumination using Ag, Al and Au electrodes, which can be fitted very well with Equation 3. The responsivity increases with the decrease of light illumination and shows a nonlinear relationship similar to the reports on other photodetectors.[25, 29] The fitting parameters for Ag and Al contacts are approximate equal, while have a large difference compared with Au contact, indicating intrinsically different contact type. The low responsivity of Au contact can attribute to low photocurrent from Schottky contact. However, the calculated on/off ratio at 1 V bias of Au contact is 146, which is larger than Al contact of 87. Besides, the response and recovery times are nearly same for both Al and Au contacts under high light illumination. (Fig. S6 and S7). These results indicate that Schottky contact has not obtained higher responsivity and faster response and recovery speeds than Ohmic contact, which is different with previous reports.[35, 36, 39] One reason is that our polycrystalline ZnO thin films have much higher density of surface states at the contact interface compared with single ZnO NWs, which

significantly modify the barrier of Schottky contact. The another reason may be that Au has diffused into Ag NWs embedded in ZnO NPs thin films during the sputtering process due to very thin layer of upper ZnO NPs, which reduced the effect of Schottky contact. These suppose can be partially supported by the microphotograph in Fig. S3b. The wavelength-dependent responsivity was calculated from the incident photon-to-current conversion efficiency (IPCE) measured using a model 7-SCSpec II system and the expression $R(\lambda)=1240*IPCE/\lambda$. From Fig. 5 (d), we can obtain UV to visible rejection ratio of 40, which intrinsically ensures so-called "visible-blind" property of UV photodetector. Compared with ZnO photodiode detector reported elsewhere,[41,42] this rejection ratio is not good enough. We think the IPCE measurements under high light power have severe thermal effect, which produces large photocurrent even under visible spectrum. This is also in accordance with the result mentioned above, which means that the responsivity decreases with the increase of light illumination. In all, our ZnO/Ag NWs/ZnO composite structure has greatly improved the UV photoresponse performance of polycrystalline ZnO thin films, thus it reduces the performance dependence on electrode contact.

3. Conclusion

In summary, high-performance ZnO/Ag NWs/ZnO composite UV photodetectors have been fabricated using solution-processed method. The large photosensitive area of $4\times5mm^2$, low operating voltage of 1 V and high visible transmittance of 75% can be achieved using simple and low-cost processing condition, which suggests an potential in large area UV photodetective applications. Under high light illumination

of 4.9mW/cm^2, the device shows high photocurrent of 41.8μA and large on/off ratio of 2787, and short response and recovery times of 3.5 s, which is adequate for applications that do not require particularly high speeds. On the opposite, the device shows large detectivity of 6.8×10^{12} Jones and responsivity of 2.4 A/W under low light illumination of 10μW/cm^2, indicating excellent weak light detection capability of composite UV photodetectors. Besides, the device also shows good linear dynamic range of 64 dB, which is very close to InGaAs photodetectors. The obtained high performance can be explained by that Ag NWs conductive network embedded in polycrystalline ZnO thin films plays a role in suppressing the recombination of photogeneration excitons and rapidly transferring photoelectrons in ZnO NPs. This will not only greatly improve the extraction number of photoelectrons, but also shorten extraction time of polycrystalline thin films. We also find that both Schottky contact and Ohmic contact at the electrode interface can obtain high on/off ratio and short response and recovery times. It is effective composite structure that reduces the performance dependence on electrode contact.

4. Experimental details

Fabrication of bottom ZnO layer

Bottom ZnO layer was prepared on the clean glass substrate by the conventional sol-gel spin-coating method.[43] The zinc acetate precursor solution was spin-coated onto glass substrate at 4000 rpm. Then the films were dried at 300 ℃ for 10 min to remove organic residuals. Next, the procedure from spin-coating to drying was

repeated from once to four times in order to get different amounts of bottom ZnO layer.

Fabrication of ZnO/Ag NWs/ZnO composite UV photodetector

Ag NWs were synthesized using Xia's method.[44] 5 mg/ml of Ag NWs ethanol ink was got by adding appropriate amounts of PVP to adjust the dispersity and viscosity. Then Ag NWs ethanol ink was spin-coated onto bottom ZnO layer prepared above at different spin speeds to get different Ag NWs density. Next, the films were treated at 200 ℃ for 20 min to improve conductivity. Finally, the 6-nm-diameter ZnO nanoparticles were synthesized according to literature methods.[45] Then the upper ZnO layer was prepared by spin-coating as-synthesized ZnO nanoparticles onto films prepared above. Then three kinds of metal electrodes were prepared onto composite films surface to make different contacts. Ag, Al and Au electrodes with 4-mm-spacing were sputtering through a shadow mask. The length and width of three kinds of electrodes are 5 mm and 1.5mm, respectively.

Characterizationm

Surface morphologies with high magnification were taken with FEI Quatan 250 FEG scanning electron microscope (SEM), and low magnification morphologies with large view field were performed on Olympus BX 51 Microscope System. TEM tests were performed on a JEOL1400 with an accelerating voltage of 100 kV. Optical transmittance data were acquired with a Jasco V-570 UV/Visible spectrophotometer. IV and time-dependent photoresponse measurements were recorded by Keithley 2400 source meter. The samples were illuminated through a mercury arc lamp (Starsense,

GGY-125). The light intensity was modulated by changing distance between light source and sample, and a standard silicon diode UV of 365 nm (Photoelectric Instrument Factory of Beijing Normal University, UV-A) was used to quantify UV irradiance.

Acknowledgements

This work has been partially supported by the NSFC Major Research Plan on Nanomanufacturing (Grant No. 91323303). The authors gratefully acknowledge financial support from Natural Science Foundation of China (Grant Nos. 91123019 and 61176056), 111 program (No. B14040) and the open projects from Institute of Photonics and Photo-Technology, Provincial Key Laboratory of Photoelectronic Technology, Northwest University, China.

References

1 Y. Z. Jin, J. P. Wang, B. Q. Sun, J. C. Blakesley and N. C. Greenham, *Nano Lett.* 2008, **8,** 1649-1653.
2 E. Monroy, F. Omnes and F. Calle, *Semicond. Sci. Technol.* 2003, **18,** R33-51.
3 E. Monroy, F. Calle, J. L. Pau, E. Muñoz, F. Omnès, B. Beaumont and P. Gibart, *J. Cryst. Growth* 2001, **230,** 537-543.
4 K. Liu, M. Sakurai, and M. Aono, *Sensors* 2010, **10,** 8604-8634.
5 W. Tian, T. Y. Zhai, C. Zhang, S. L. Li, X. Wang, F. Liu, D. Q. Liu, X. K. Cai, K. Tsukagoshi and D. Golberg, *Adv. Mater.* 2013, **25,** 4625-4630.
6 H. Kind, H. Q. Yan, B. Messer, M. Law and P. D. Yang, *Adv. Mater.* 2002, **14,** 158-160.
7 S. Bai, W. W. Wu, Y. Qin, N. Y. Cui, D. J. Bayerl and X. D. Wang, *Adv. Funct. Mater.* 2011, **21,** 4464-4469.
8 Y. K. Su, S. M. Peng, L. W. Ji, C. Z. Wu, W. B. Cheng and C. H. Liu, *Langmuir* 2010, **26,** 603-606.
9 S. M. Peng, Y. K. Su, L. W. Ji, C. Z. Wu, W. B. Cheng and W. C. Chao, *J. Phys. Chem. C* 2010, **114,** 3204-3208.
10 S. Liu, J. F. Ye, Y. Cao, Q. Shen, Z. F. Liu, L. M. Qi and X. F. Guo, *Small* 2009, **5,** 2371-2376.
11 C. Soci, A. Zhang, B. Xiang, S. A. Dayeh, D. Aplin, J. Park, X. Y. Bao, Y. H. Lo and D. Wang, *Nano Lett.* 2007, **7,** 1003-1009.

12 S. W. Lee, M. C. Jeong, J. M. Myoung, G. S. Chae and I. J. Chung, *Appl. Phys. Lett.* 2007, **90,** 133115.
13 A. Afal, S. Coskun and H. Emrah Unalan, *Appl. Phys. Lett.* 2013, **102,** 043503.
14 J. Z. Li, J. Y. Lin, H. X. Jiang and M. A. Khan, *Appl. Phys. Lett.* 1998, **72,** 2868.
15 Z. Yang, M. Q. Wang, Y. H. Shi, X. H. Song, Z. H. Lin, Z. Y. Ren and J. T. Bai, *J. Mater. Chem.* 2012, **22,** 21009-21016.
16 Z. H. Lin, M. Q. Wang, L. Y. Zhang, Y. H. Xue, X. Yao, H. W. Cheng and J. T. Bai, *J. Mater. Chem.* 2012, **22,** 9082-9085.
17 D. D. Lin, H. Wu, W. Zhang, H. P. Li and W. Pan, *Appl. Phys. Lett.* 2009, **94,** 172103.
18 S. K. Tzeng, M. H. Hon and I. C. Leu, *J. Electrochem. Soc.* 2012, **159,** H440-443.
19 K. Liu, M. Sakurai, M. Y. Liao and M. Aono, *J. Phys. Chem. C* 2010, **114,** 19835-19839.
20 Z. X. Wang, X. Y. Zhan, Y. J. Wang, S. Muhammad, Y. Huang and J. He, *Nanoscale* 2012, **4,** 2678-2684.
21 X. W. Fu, Z. M. Liao, Y. B. Zhou, H. C. Wu, Y. Q. Bie, J. Xu and D. P. Yu, *Appl. Phys. Lett.* 2012, **100,** 223114.
22 R. M. Mutiso, M. C. Sherrott, A. R. Rathmell, B. J. Wiley and K. I. Winey, *ACS nano* 2013, **7,** 7654-7663.
23 A. Kim, Y. Won, K. Woo, C. H. Kim and Jooho, *ACS nano* 2013, **7,** 1081-1091
24 F. S. Morgenstern, D. Kabra, S. Massip, T. J. Brenner, P. E. Lyons, J. N. Coleman and R. H. Friend, *Appl. Phys. Lett.* 2011, **99,** 183307.
25 Z. H. Sun, Z. K. Liu, J. H. Li, G. a. Tai, S. P. Lau and F. Yan, *Adv. Mater.* 2012, **24,** 5878-5883.
26 G. Konstantatos, M. Badioli, L. Gaudreau, J. Osmond, M. Bernechea, F. P. G. de Arquer, F. Gatti and F. H. Koppens, *Nat. Nanotechnol.* 2012, **7,** 363-368.
27 K. K. Manga, J. Z. Wang, M. Lin, J. Zhang, M. Nesladek, V. Nalla, W. Ji and K. P. Loh, *Adv. Mater.* 2012, **24,** 1697-1702.
28 X. Gong, M. H. Tong, Y. J. Xia, W. Z. Cai, J. S. Moon, Y. Cao, G. Yu, C. L. Shieh, B. Nilsson and A. J. Heeger, *Science* 2009, **325,** 1665-1667.
29 G. Konstantatos, I. Howard, A. Fischer, S. Hoogland, J. Clifford, E. Klem, L. Levina and E. H. Sargent, *Nature* 2006, **442,** 180-183.
30 J. P. Clifford, G. Konstantatos, K. W. Johnston, S. Hoogland, L. Levina and E. H. Sargent, *Nat. Nanotechnol.* 2008, **4,** 40-44.
31 H. Zhu, C. X. Shan, L. K. Wang, J. Zheng, J. Y. Zhang, B. Yao and D. Z. Shen, *J. Phys. Chem. C* 2010, **114,** 7169-7172.
32 J. W. Liu, R. T. Lu, G. W. Xu, J. Wu, P. Thapa and D. Moore, *Adv. Funct. Mater.* 2013, **23,** 4941-4948.
33 P. Sharma, K. Sreenivas and K. V. Rao, *J. Appl. Phys.* 2003, **93,** 3963-3970.
34 Y. B. Li, F. Della Valle, M. Simonnet, I. Yamada and J. J. Delaunay, *Nanotechnology* 2009, **20,** 045501.
35 J. Zhou, Y. D. Gu, Y. F. Hu, W. J. Mai, P. H. Yeh, G. Bao, A. K. Sood, D. L. Polla and Z. L. Wang, *Appl. Phys. Lett.* 2009, **94,** 191103.

36 Y. F. Hu, J. Zhou, P. H. Yeh, Z. Li, T. Y. We and Z. L. Wang, *Adv. Mater.* 2010, **22,** 3327-3332.
37 J. H. Song, J. Zhou and Z. L. Wang, *Nano Lett.* **2006**, *6*, 1656-1662.
38 H. K. Kim, K. K. Kim, S. J. Park, T. Y. Seong and I. Adesida, *J. Appl. Phys.* 2003, **94,** 4225-4227.
39 G. Cheng, X. H. Wu, B. Liu, B. Li, X. T. Zhang and Z. L. Du, *Appl. Phys. Lett.* 2011, **99,** 203105.
40 F. Yan, J. H. Li and S. M. Mok, *J. Appl. Phys.* 2009, **106,** 074501.
41 O. Game, U. Singh, T. Kumari, A. Banpurkar, and S. Ogale, *Nanoscale* 2014, **6,** 503-513.
42 S. M. Hatch, J. Briscoe, and S. Dunn, *Adv. Mater.* 2013, **25,** 867–871.
43 J. P. Deng, M. Q. Wang, X. H. Song, Y. H. Shi and X. Y. Zhang, *J. Colloid Interface Sci.* 2012, **388,** 118-122.
44 B. Wiley, Y. G. Sun and Y. N. Xia, *Langmuir* 2005, **21,** 8077-8080.
45 B. Q. Sun and H. Sirringhaus, *Nano Lett.* 2005, **5,** 2408-2413.

Figure captions

Figure 1. (a) Schematic of ZnO/Ag NWs/ZnO composite UV photodetector device structure SEM images of composite UV photodetector between two electrodes: (b) Plan view. (c) Magnified view of Ag NWs junction. (d) Cross section. The thickness of bottom ZnO NPs thin film is about 200 nm.

Figure 2. (a) IV curves of ZnO/Ag NWs/ZnO composite UV photodetector with and without UV light illumination. Inset is IV curves of UV photodetector with and without UV light illumination, which has same condition but no middle Ag NWs layer. (b) The dependence of photocurrent and on/off ratio on spin speed of Ag NWs. (c) The dependence of photocurrent and on/off ratio on thickness of bottom ZnO layer. Photocurrents were obtained at 1 V applied bias under UV light illumination of 10μW/cm^2. (d) The transmittance spectrum of several UV photodetectors with different process condition. The air baseline is subtracted for all samples to get accurate transmittance value. Inset is the picture of composite UV photodetector with Au electrodes.

Figure 3. (a) IV curves of ZnO/Ag NWs/ZnO composite UV photodetector with optimized processing condition under different light illumination. (b) Photocurrent and detectivity versus light illumination measured at 1 V applied bias, revealing good linearity. (c) Time-dependent photoresponse at 1 V applied bias under 4.9 mW/cm^2 of light illumination. Experimental curves and exponential fitting curves of photocurrent rising and decay process are shown. (d) Time-dependent photoresponse at 1 V applied bias under different light illumination.

Figure 4. (a) Schematic illustrations of the energy band structure of forming heterojunction between Ag NWs and ZnO NPs, indicating effective ohmic contact. (b) Schematic illustrations of carrier transfer process at the interface between Ag NWs and ZnO NPs and inside ZnO NPs. The electrons were represented by red dots, and holes were represented by blue dots.

Figure 5. (a) and (b) are IV curves of ZnO/Ag NWs/ZnO composite UV photodetectors at the optimized processing condition with Al electrodes and Au electrodes under different light illumination, respectively. (c) Responsivity measured at 1 V applied bias for composite UV photodetectors versus light illumination using Ag, Al and Au electrodes. Inset is fitting parameters α and β. (d) Spectral responsivity of composite UV photodetector under optimized processing condition.

Table 1. The performance comparison of UV photodetector based on different ZnO structures.

Device	Active area (mm^2)	On/off ratio	Responsivity (A/W)	Recovery time (s)	Voltage (V)	Light intensity (mW/cm^2)	Reference
ZnO NPs films	0.24×3	10^6	61	9	120	1.06	1
ZnO NPs films	0.15×0.16	285	0.13	2.42	5	18	7
Integrated ZnO NW	10×26	83000	0.09	14	1	4.5	6
ZnO NWs arrays	0.15×0.16	3000	41.22	15.44	5	18	7
ZnO nanobridge	0.008×0.08	7770	167	2.54	5	57	8
ZnO NP/SWCNT	10^{-5}×0.02	18	3.05×10^5	—	0.005	0.026	9
ZnO NP/RGO	5×10	116	0.0013	3.5	10	1.5	19
Vertical G/ZnO/G	0.012×0.07	800	—	0.5	3	0.1	20
ZnO/Ag NWs/ZnO	4×5	2787	0.1	3.67	1	4.9	this work

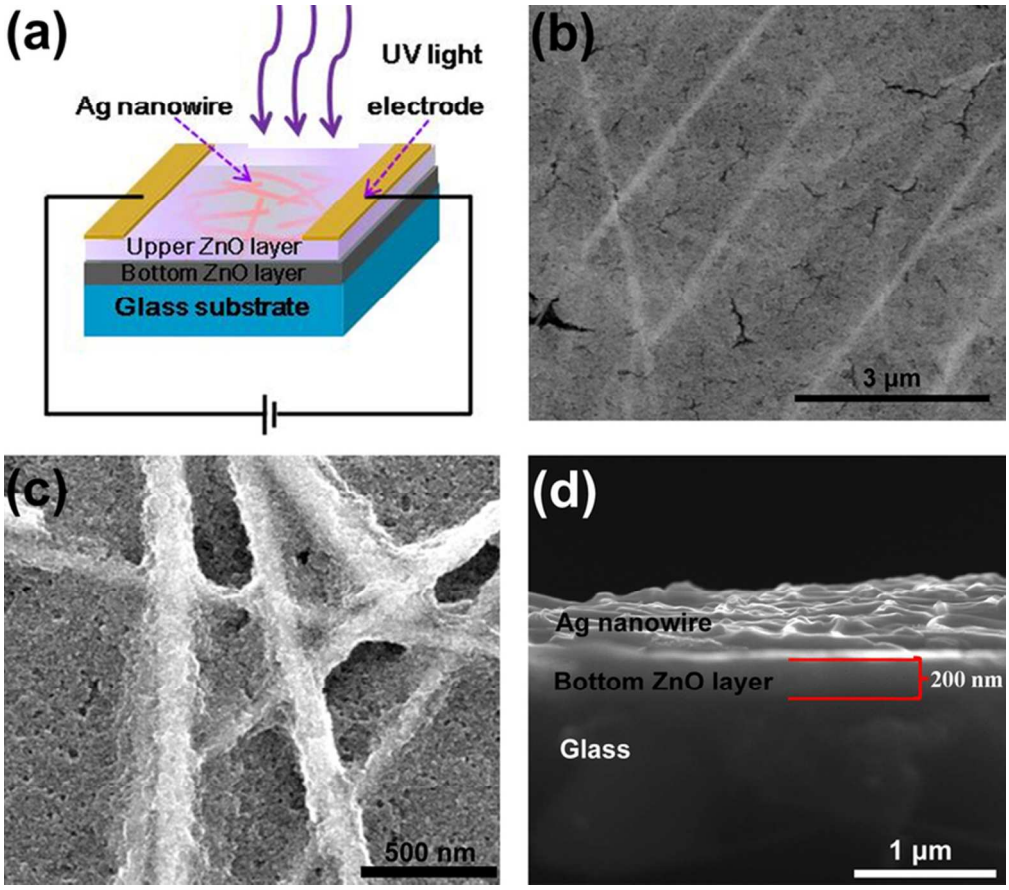

70x61mm (300 x 300 DPI)

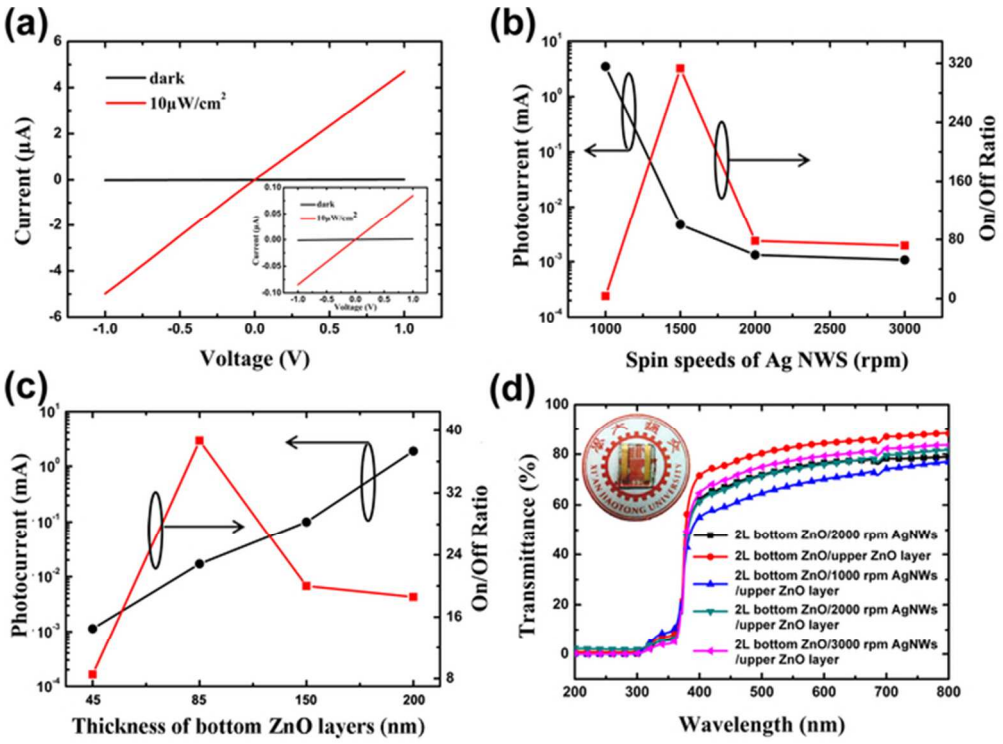

58x43mm (300 x 300 DPI)

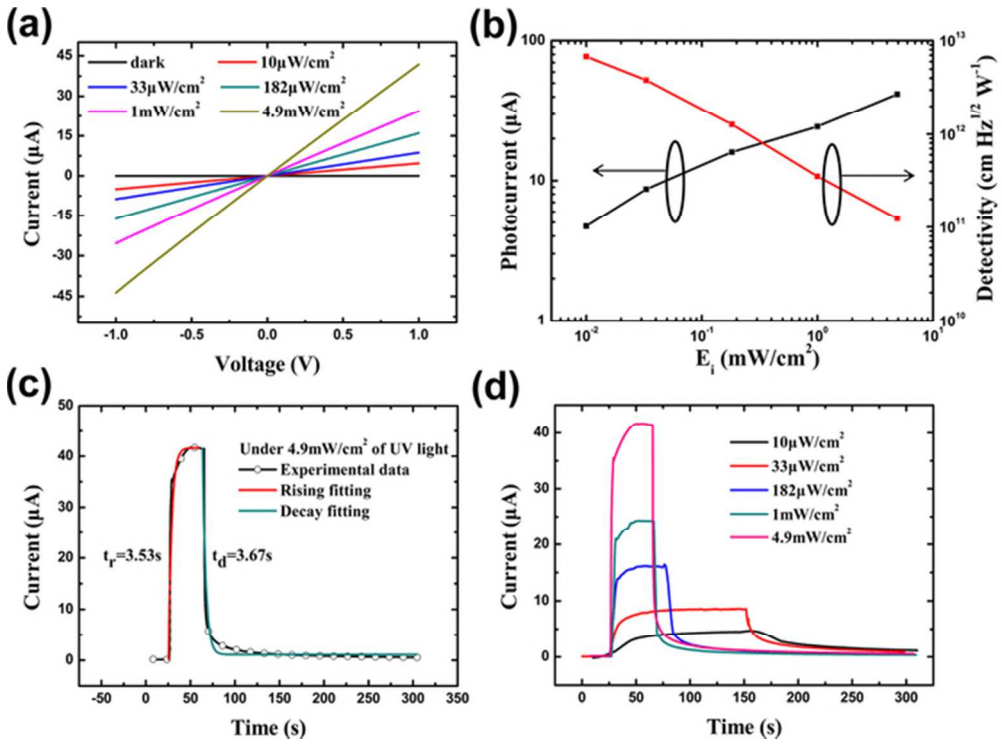

58x42mm (300 x 300 DPI)

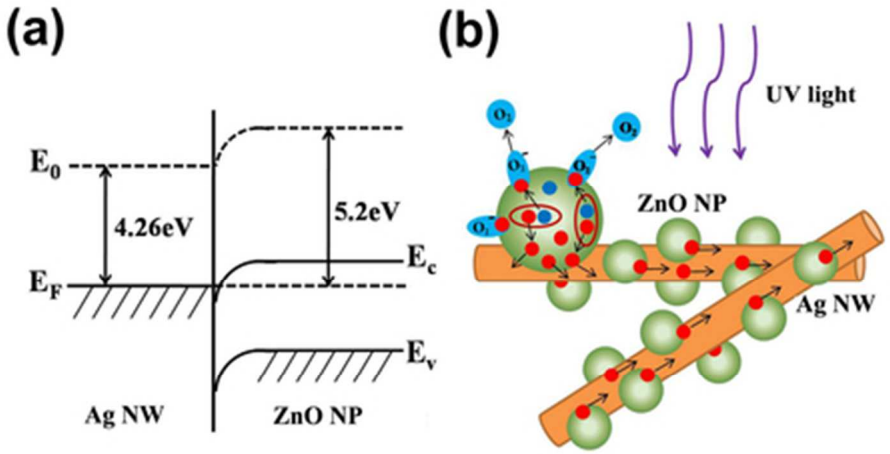

39x19mm (300 x 300 DPI)

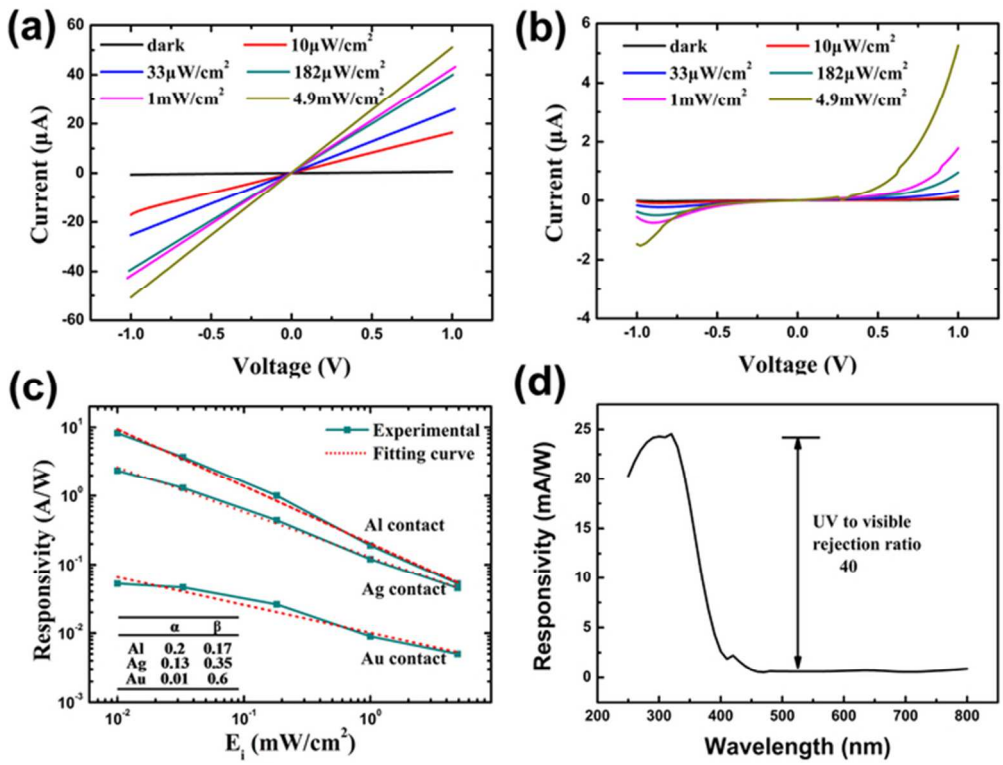

60x46mm (300 x 300 DPI)

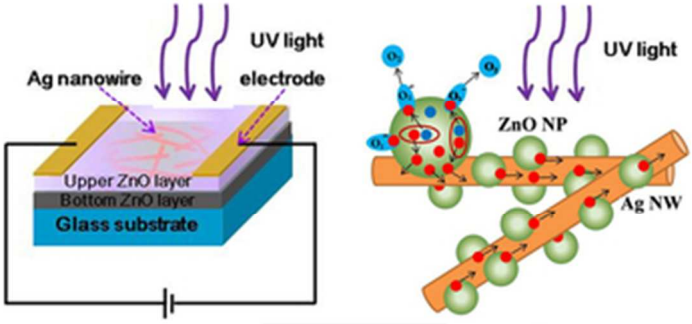

We have demonstrated the important role of the inserted Ag nanowires network to greatly improve responsivity and shorten response time in ZnO/Ag Nanowires/ZnO Composite UV photodetector.
29x14mm (300 x 300 DPI)